

Probing sunspot magnetic fields with p-mode absorption and phase shift data

P. S. Cally,^{1,2★†} A. D. Crouch^{1★} and D. C. Braun^{3★}

¹Centre for Stellar and Planetary Astrophysics, School of Mathematical Sciences, Monash University, Victoria 3800, Australia

²High Altitude Observatory, National Centre for Atmospheric Research, PO Box 3000, Boulder, CO 80307-3000, USA

³NorthWest Research Associates, Inc., Colorado Research Associates Division, 3380 Mitchell Lane, Boulder, CO 80301-5410, USA

Accepted 2003 July 11. Received 2003 July 11; in original form 2003 May 13

ABSTRACT

Long-standing observations of incoming and outgoing f- and p-modes in annuli around sunspots reveal that the spots partially absorb and substantially shift the phase of waves incident upon them. The commonly favoured absorption mechanism is partial conversion to slow magneto-acoustic waves that disappear into the solar interior channelled by the magnetic field of the sunspot. However, up until now, only f-mode absorption could be accounted for quantitatively by this means. Based on vertical magnetic field models, the absorption of p-modes was insufficient. In this paper, we use the new calculations of Crouch & Cally for inclined fields, and a simplified model of the interaction between spot interior and exterior. We find excellent agreement with phase shift data assuming field angles from the vertical in excess of 30° and Alfvén/acoustic equipartition depths of around 600–800 km. The absorption of f-modes produced by such models is considerably larger than is observed, but consistent with numerical simulations. On the other hand, p-mode absorption is generally consistent with observed values, up to some moderate frequency dependent on radial order. Thereafter, it is too large, assuming absorbing regions comparable in size to the inferred phase-shifting region. The excess absorption produced by the models is in stark contrast with previous calculations based on a vertical magnetic field, and is probably due to finite mode lifetimes and excess emission in acoustic glories. The excellent agreement of phase shift predictions with observational data allows some degree of probing of subsurface field strengths, and opens up the possibility of more accurate inversions using improved models. Most importantly, though, we have confirmed that slow mode conversion is a viable, and indeed the likely, cause of the observed absorption and phase shifts.

Key words: Sun: helioseismology – Sun: magnetic fields – sunspots.

1 INTRODUCTION

One method of determining how solar oscillations interact with sunspots and other magnetic field concentrations was developed by Braun, Duvall & LaBonte (1987) (see also Braun et al. 1992; Bogdan et al. 1993; Braun 1995; Zhang 1997), who observed ingoing and outgoing waves in annuli surrounding spots and plage. This has come to be called Hankel analysis, because of the decomposition into ingoing and outgoing Hankel functions used in most cases. Their unanticipated finding was that sunspots *absorb* up to half of the incident p-mode power at favoured frequencies and horizontal wavenumbers.

More recently, new local helioseismic techniques have been used to probe sunspots and their surroundings. For example, acoustic holography has confirmed the Hankel analysis results (Lindsey & Braun 1999; Braun & Lindsey 2000a; Chou 2000), adding in particular fascinating information concerning enhanced acoustic emission in regions surrounding sunspots (acoustic glories) (Donea, Lindsey & Braun 2000; Jain & Haber 2002). Acoustic tomography, also known as time–distance helioseismology, has similarly been very successful at imaging subspot regions. (see the well-known ‘coffee mug’ image from the *SOHO-9* workshop; Kosovichev, Duvall & Scherrer 2000, fig. 8). Unlike Hankel analysis, tomography and holography dispense with a modal description altogether in favour of ray or optics formalisms, and are very adept at directly imaging subsurface thermal and flow features. However, despite some progress (Kosovichev & Duvall 1997; Kosovichev, Duvall & Scherrer 2000, 2001), as yet neither holography nor tomography treats magnetic fields entirely satisfactorily. For example, only the

*E-mail: paul.cally@sci.monash.edu.au (PSC); ashley.crouch@maths.monash.edu.au (ADC); dbraun@cora.nwra.com (DCB)

†The National Centre for Atmospheric Research is sponsored by the National Science Foundation.

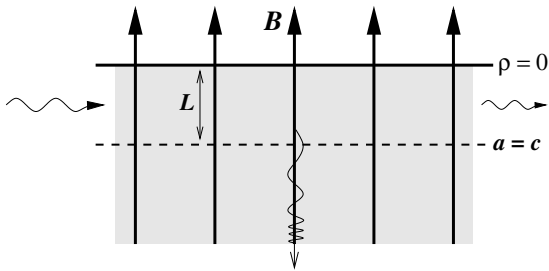


Figure 1. Schematic diagram showing an acoustic wave incident on a vertical magnetic field concentration from the left, and being partially transmitted and partially converted to slow modes, which travel down the magnetic field lines. In reality, there will also be some reflection and scattering. The depth at which the sound and Alfvén speeds coincide is denoted by L . In the simple polytropic model adopted in this paper, the density vanishes at the surface.

fast magnetoacoustic wave is retained in Kosovichev & Duvall (1997), Section 2.3, and Kosovichev et al. (2000), Section 2.4, and despite the theoretical possibility of disentangling sound and Alfvén speeds, only their sum has so far been reliably measured. (Further questions concerning the treatment of the acoustic cut-off and Brunt-Väisälä frequencies in the ray approach are discussed by Barnes & Cally 2001).

Indeed, the tomography assumption of a single ray speeding up or slowing down as it meets various features is not appropriate to the mode conversion process commonly envisaged as the cause of wave absorption in sunspots. As first suggested by Spruit (1991) and Spruit & Bogdan (1992), and developed by Cally & Bogdan (1993), Cally, Bogdan & Zweibel (1994), Bogdan & Cally (1997) and Cally (2000), when a p-mode encounters magnetic field concentrations characteristic of sunspots, it splits into ‘fast’ and ‘slow’ waves that are quite different in nature. Indeed, this coupling is expected to be strongest where the speed of sound c and Alfvén speed a are comparable, in which case the distinction between fast and slow is small. Below this shallow depth though, the speed of sound greatly exceeds the Alfvén speed and the two modes decouple. They are then clearly distinguishable: the fast wave is essentially acoustic, and behaves very much like the p-mode (it is termed the π -mode by Cally & Bogdan 1993), and the slow mode is nearly transverse, has a wavelength that decreases with depth, and behaves much like an Alfvén wave. This scenario is depicted schematically in Fig. 1.

Although the vertical field model predicts that f-modes are substantially absorbed (Cally et al. 1994), p-modes of increasing radial order are progressively too weakly affected to account for observations. Based on two-dimensional Cartesian simulations, Cally (2000) suggested that a spreading magnetic field, as found in sunspots, might be more effective. However, it was unclear whether it was the spreading of the field that had the desired effect, or merely its inclination away from the vertical. To explore this question, Crouch & Cally (2003) calculated the eigenfunctions and complex eigenvalues of oscillations in an adiabatic polytropic model of index $m_p = 1.5$ (i.e. $\gamma = \frac{5}{3}$) with uniform inclined magnetic field, and found that indeed substantial enhancements in absorption were found as the field was rotated away from the vertical, with a peak effect at around 30° .

It is the purpose of this paper to explore the extent to which the inclined field results of Crouch & Cally (2003) can quantitatively explain the Hankel observations. To that end, we shall compare with the absorption and phase shift results presented in Braun (1995), which still represents the highest-quality data set of its type. Two sunspot groups, NOAA5254 and NOAA5229 are examined in detail

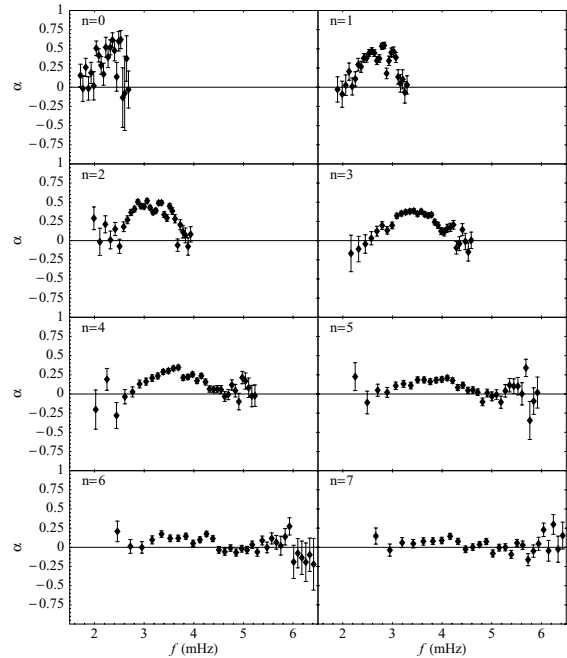


Figure 2. Absorption coefficient α versus frequency for the f- and p-modes in the spot NOAA5254 for different radial order n . The f-mode corresponds to $n = 0$. This figure is a replotting of fig. 4 of Braun (1995), though against frequency rather than spherical degree ℓ . The entire data set is used, i.e. $61 \leq \ell \leq 720$. Error bars in this and other figures are those of Braun (1995).

in that reference, each using long data sets collected at the South Pole in 1988 (Braun et al. 1992). The former contains a large nearly circular spot with an umbral radius of 9 Mm and a penumbral radius of 18 Mm. The primary spot in NOAA5229 is slightly smaller and less regular. Since the absorption and phase shift results for each are very similar, we shall focus on NOAA5254 here. The annulus used for the Hankel analysis had an inner radius of 30 Mm and an outer radius of 243 Mm. The absorption coefficient α for NOAA5254 is plotted against frequency in Fig. 2, illustrating the points that:

- (i) α rises from zero at low frequency to a maximum value and then dips to zero before apparently rising again (see $n = 3-5$ in particular);
- (ii) peak absorption diminishes with increasing radial order;
- (iii) the frequency of the absorption dip is around 5 mHz at larger radial order, but is lower at lower n .

Any successful model should reproduce these features.

2 MODEL

Tables resulting from the model of Crouch & Cally (2003) present the complex eigenvalues κ against real dimensionless frequency ν in a complete adiabatic polytrope of index $m_p = 1.5$ with magnetic inclination angle $\theta = 0^\circ, 5^\circ, 10^\circ, \dots, 55^\circ$ and p-mode radial index $n = 0, 1, \dots, 8$ (higher angles are also available, but are not complete in n). Here

$$\nu = \sqrt{\frac{m_p L}{g}} \omega, \quad (1)$$

where g is the gravitational acceleration, L is the depth at which the sound and Alfvén speeds coincide and $\kappa = 2kL$ is a dimensionless horizontal wavenumber. In Cartesian geometry, we have assumed an $\exp[i(kx - \omega t)]$ dependence on horizontal position x and time t .

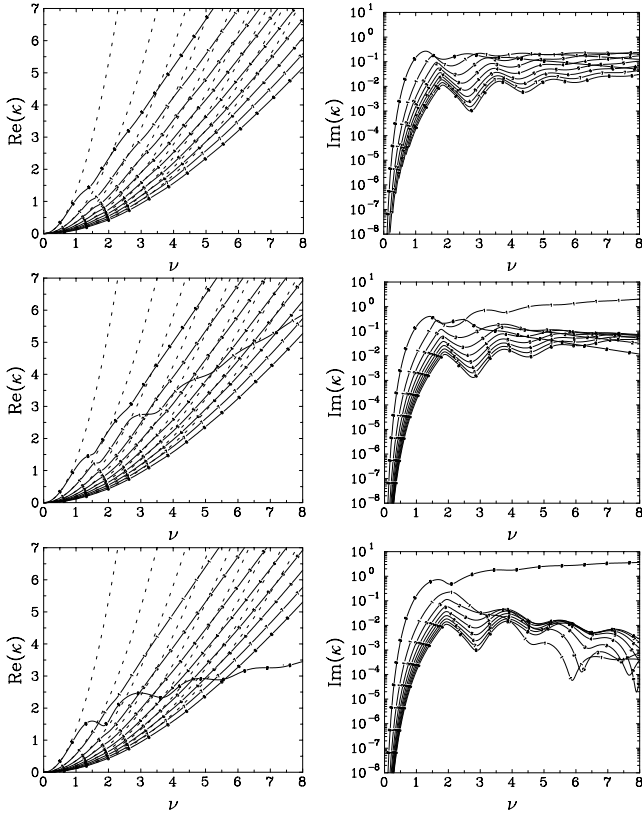


Figure 3. The real (left-hand panels) and imaginary (right-hand panels) parts of the eigenvalues κ against non-dimensional frequency ν for the complete $m_p = 1.5$ adiabatic polytrope with uniform magnetic field at angle $\theta = 30^\circ$ and $\phi = 0^\circ$ (top panels), $\phi = 45^\circ$ (middle panels) and $\phi = 90^\circ$ (bottom panels). In the left-hand panels, the dashed lines represent the non-magnetic case, and correspond to the f-, p_1 , ..., p_8 -modes, respectively, from left to right.

Although the eigenvalue tables of Crouch & Cally (2003) are calculated for a uniform field distribution without bounds, the essence of the model we develop in this paper is to adopt the eigenvalues κ globally, i.e. to assume that the damping parameter $\text{Im}(\kappa)$ and the local wavenumber $\text{Re}(\kappa)$ given by these calculations applies (at least on average) to the spot as a whole, though the field is of course not uniform throughout. [In Section 3.1 we shall indeed adopt a single value of inclination angle θ and equipartition depth L to be representative of the whole spot, but in Section 3.2 we relax this by allowing for a nested set of piecewise uniform shells. Experience with a two-dimensional (2D) numerical code (Cally 2000) indicates that absorption and phase shifting are localized over a shallow depth of less than about 1 Mm beneath the spot, and so variation of θ with depth is not important.]

For the vertical field, the same equations (and solutions) as are addressed in Cally & Bogdan (1993) and Cally et al. (1994) also result from a cylindrical decomposition in which the three components of velocity take the form (Scheuer & Thomas 1981)

$$\begin{aligned} u_r &= U(z) \left[k Z_{m+1}(kr) - \frac{m}{r} Z_m(kr) \right] \exp[i(m\vartheta - \omega t)], \\ u_\vartheta &= -imU(z) \frac{Z_m(kr)}{r} \exp[i(m\vartheta - \omega t)], \\ u_z &= -ikW(z) Z_m(kr) \exp[i(m\vartheta - \omega t)], \end{aligned} \quad (2)$$

where Z represents a Bessel function or linear combination of them [J , Y or the Hankel functions $H^{(1,2)}$] as appropriate.

In Cartesian geometry, it is assumed that the inclination θ of the uniform magnetic field lies in the x - z plane (the ‘fourth-order’ problem, because the Alfvén wave decouples in this case leaving a fourth-order system of governing differential equations). Extension to full three-dimensionality (the ‘sixth-order’ problem), where \mathbf{B} makes an angle ϕ with this plane, reveals that the dependence of κ on ϕ is generally weak compared with that on θ (Crouch & Cally, in preparation), and we shall ignore it in the simple model presented here. To illustrate the point, Fig. 3 shows the real and imaginary parts of the eigenvalue κ against dimensionless frequency ν for the case $\theta = 30^\circ$ (where absorption is approximately maximal) and various values of ϕ . It turns out that we are mainly interested in the behaviour for $\nu \lesssim 3$, where ϕ indeed makes little difference, apart from the case of $\text{Re}(\kappa)$ for the p_1 -mode ($\phi = 45^\circ$) and the f-mode ($\phi = 90^\circ$). Since the observational data for f-mode phase shifts is too noisy to be useful, this $\text{Re}(\kappa)$ dependence on ϕ does not affect any comparisons we shall make involving the fundamental mode. It may have more effect on p_1 at intermediate ϕ though.

The cylindrical geometry analogue strictly would be a straight-field conical structure (Cally 1983), where θ increases linearly with r , and only with radial ($m = 0$) oscillations in the 2D case. However, in the spirit of exploration (and since this is a very difficult problem to solve), we assume a uniform θ throughout the magnetic region, or piecewise uniform in cylindrical shells, and simply adopt the κ eigenvalues from Crouch & Cally (2003). The essential idea is that κ is a global property of a cylindrical spot, to be read from tables, under the assumption that equations (2) are valid. The magnetic field plays no other role than to supply these κ .

In the inner shell, Z_m must be the J_m Bessel function for the solution to be bounded at $r = 0$, whilst in the outer non-magnetic region, it is a linear combination,

$$Z_m(kr) = A H_m^{(1)}(kr) + H_m^{(2)}(kr)$$

corresponding to outgoing and incoming waves, respectively. An arbitrary normalization has been applied in which the amplitude of the incoming wave is unity. In any intervening shells, Z_m is an arbitrary combination of J_m and Y_m . Each shell has its own complex k , read from tables. The total pressure and the radial velocity is matched across each shell boundary $r = R_i$ ($0 < R_1 < \dots < R_N = R$), i.e. $Z_m(kr)$ and $dZ_m(kr)/dr$, respectively. This allows all the coefficients in the Bessel linear combinations to be determined. Then, from A , we calculate the absorption coefficient α and the phase shift δ using

$$\alpha = 1 - |A|^2, \quad \delta = -\arg(A). \quad (3)$$

An advance in phase ($\delta > 0$) represents an *increase* in phase speed through the spot. Note that if the internal wavenumber k is the same as that in the external region, k_0 (real), then $A = 1$ and $\alpha = \delta = 0$ as expected.

Limitations of the model are:

- (i) the magnetic field geometry has been simplified to be piecewise uniform;
- (ii) the magnetic field variation with depth is not included;
- (iii) the dependence of κ on the angle ϕ is ignored;
- (iv) scattering across radial order n has been neglected (see the discussions in Braun 1995; Barnes & Cally 2000);
- (v) the acoustic jacket has been ignored (Bogdan & Cally 1995; Barnes & Cally 2000);
- (vi) an $m_p = 1.5$ planar polytrope has been used to calculate the complex κ , though we partially correct for it through the p-mode ridge adjustment procedure discussed later in this section;

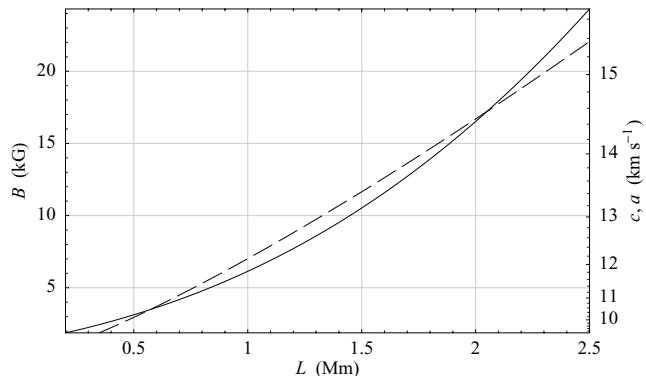


Figure 4. Magnetic field strength B against equipartition depth L for a uniform field in (i) full curve: the realistic solar model fgong.l5bi.d.15 from the Aarhus adiabatic pulsation package (Christensen-Dalsgaard 1997), and (ii) dashed curve: a complete adiabatic polytrope of index $m_p = 1.5$, assuming a density at 1 Mm taken from the Aarhus model. The right-hand axis shows the sound and Alfvén speeds at this equipartition depth in the Aarhus model only.

(vii) the difference in thermal structure inside and outside the spot has not been explicitly included;

(viii) damping of acoustic emission in sunspots, and enhanced emission in acoustic glories surrounding them, are ignored;

(ix) flows are neglected; and

(x) no overlying atmosphere has been included.

Irrespective of these points, the proof of the pudding will be in the eating: despite these limitations, can Braun’s observational Hankel data be adequately matched using the model?

Several of the above points warrant further discussion. Regarding point (ii), our only measure of magnetic field strength is L , the depth in *uniform* field at which $a = c$ (see Fig. 4). In reality, we expect the magnetic field to concentrate with depth. The effect of this is that the best fit to phase shift δ and absorption coefficient α may not occur for the same L and shell radius R . The reason is that the phase speed of p- or π -modes is determined predominantly at the immediate subsurface layers (where the speed of sound is lowest), whereas absorption (conversion to slow modes) occurs somewhat lower, presumably around L . Consequently, the magnetic field strength that δ and α ‘see’ may well be different. Compounding this difference is the observational result from Hankel analysis (Braun 1995) that plage absorbs but does not scatter p-modes,¹ suggesting that the absorbing region may extend beyond the scattering region. This point is addressed further in Section 3.2.

Points (iv) and (v) are related. Because the vertical dependences of the internal and external eigenfunctions $U(z)$ and $W(z)$ are not identical, there must in reality be some degree of scattering across p-mode ridges. Our model neglects this, and by matching both u_r and total pressure, actually allows for reflection and transmission at $r = R$. When the eigenfunction mismatch is taken into account though, it turns out that it is not possible to match the interior and exterior oscillations using just the discrete sets of f- and p-modes of the given frequency in both regions. Bogdan & Cally (1995) show that a continuous spectrum of horizontally evanescent ‘jacket modes’ must also be invoked. These supply the ‘glue’ necessary to perfect the match.

¹ However, holography suggests otherwise (Braun & Lindsey 2000b). The reason for the discrepancy is unclear.

Point (x) is probably unimportant below the chromospheric acoustic cut-off frequency (~ 5 mHz), but above it a more sophisticated model should allow waves to disappear upwards as well as downwards (Cally et al. 1994).

For the single-shell model, assuming $k_0 R \gg 1$ and $\Delta k = \text{Re}(k) - k_0 \ll R^{-1}$, where k_0 is the (real) wavenumber in the outer non-magnetic region and k that inside the spot corresponding to the same frequency and p-mode ridge, the boundary matching yields

$$\delta \approx -2 \text{Re}(\Delta k)R. \quad (4)$$

For the adiabatic polytrope, for example,

$$k_0 = m_p \omega^2 / (2n + m_p)g. \quad (5)$$

From the inclined field eigenvalues (see Crouch & Cally 2003, figs 1a, 2a, 7a, and 8a), $\text{Re}(\Delta k)$ is nearly always negative, though for $\theta < 30^\circ$ it can be slightly positive at low frequency. So $\delta > 0$, and it initially grows linearly with $\text{Re}(\Delta k)$ as the frequency increases. Since k_0 increases quadratically with frequency $f = 2\pi\omega$, whilst $\text{Re}(k)$ increases only linearly, we expect a superlinear increase in δ with f . This is consistent with the Hankel data (Braun 1995). Equation (4) is also consistent with our basic understanding that an increased phase speed in the spot (decreased wavenumber) gives rise to a positive phase shift when it re-emerges. Fig. 3 shows the eigenvalues of Crouch & Cally (2003) for $\theta = 30^\circ$, showing that indeed $\text{Re}(\Delta k)$ is negative.

However, there is a complication arising from point (vi) above. Although the polytropic index has little effect on the calculated eigenvalues (see Hunter (1999) for the vertical field case), giving some reassurance about the applicability of the model of Crouch & Cally (2003) to the real sun, it does noticeably affect the location of the p-mode ridges in the f - ℓ plane. If we apply equation (5) for a given frequency $f = 2\pi\omega$, there results a considerable distortion in f . Instead, we proceed as follows: to calculate the model α and δ for a given frequency f , p-mode ridge n , and equipartition depth L , we first determine the corresponding ℓ from the real quiet sun f - ℓ curves, and hence calculate $k_0 = \sqrt{\ell(\ell+1)}/R_\odot$. Then we apply equation (5) to find the ‘polytrope-effective’ frequency, and thence ν through equation (1). The tables of Crouch & Cally are then consulted to find κ . In this way, we compensate for the discrepancy between ridge positions. Our preference for ℓ rather than f as the fundamental quantity allows us to more accurately compare the frequency dependence of α and δ with observations. If we do not apply the correction, similar results are obtained, though for larger L .

3 RESULTS

3.1 Single-shell models

The radius of the scattering region is most directly probed using a range of azimuthal degree m . The impact parameter $m R_\odot / \sqrt{\ell(\ell+1)}$ is a measure of how directly or glancingly the wave meets the spot. As this approaches the radius of the scattering region, we expect δ to drop towards zero.

To reduce error, Braun (1995) combined phase shift and absorption results into bins in ℓ centred on $\ell = 61, 82, 102, 123, 144, 164, 185, 205, 226, 246, 267, 288, 308, 329, 349, 370, 390, 411, 432, 452, 473, 493, 514, 534, 555, 576, 596, 617, 637, 658, 678, 699$ and 720. The quality of the data varies considerably across this range, with perhaps the best results at around $\ell = 288$, corresponding to a horizontal wavelength of 15.2 Mm. Fig. 5 displays the predicted phase shifts at $\ell = 288$ for a single-shell model with $L = 0.8$ Mm, $R = 27.5$ Mm, and field inclination $\theta = 30^\circ$. The comparison with

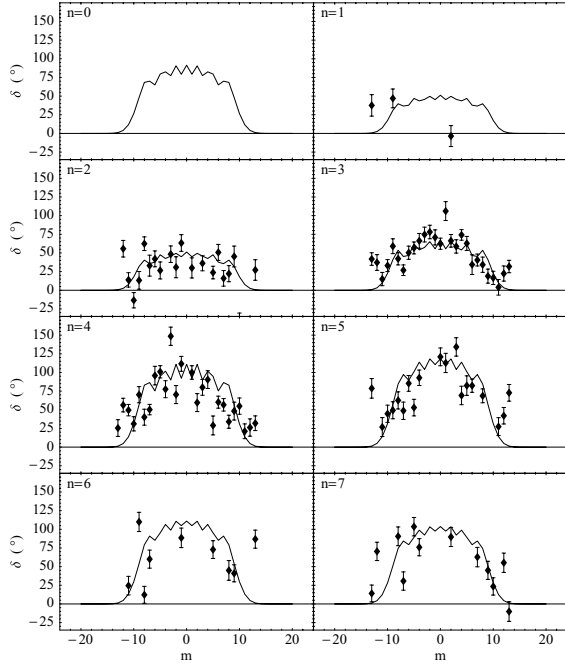


Figure 5. The predicted phase shifts δ (degrees) against angular degree m for a single-shell sunspot model with $L = 0.8$ Mm, $R = 27.5$ Mm, and $\theta = 30^\circ$ at $\ell = 288$ (full curves), for the f-mode ($n = 0$) and first seven p-modes. The points with 1σ error bars represent the Hankel analysis results (binned in ℓ about 288) for the dominant sunspot in the group NOAA5254 Braun (1995). Only points with error bars below 30° are shown.

the NOAA5254 data is impressive. Neighbouring values of L (0.6 and 1 Mm) and R (20 and 35 Mm) produce noticeably inferior fits, with $25 \lesssim R \lesssim 30$ Mm being best (cf. Fan, Braun & Chou 1995). For the most part, we shall fix on $R = 27.5$ Mm from now on.

Models with inclination angles θ below 30° yield very poor results because of the negative phase shifts they produce at some frequen-

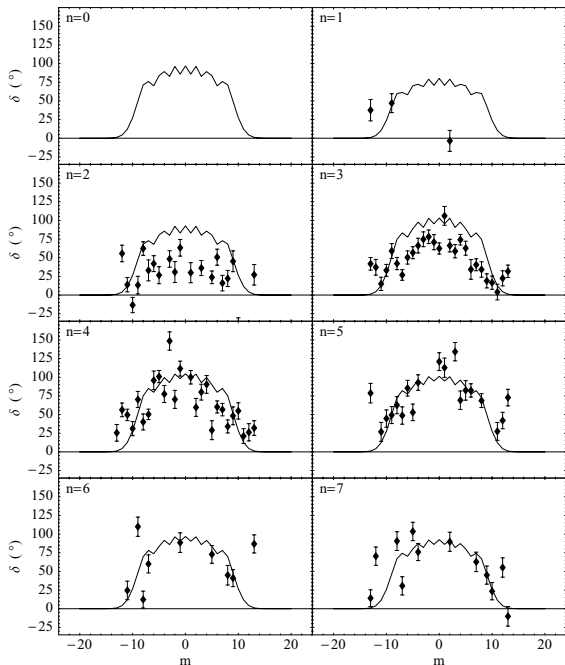


Figure 6. Same as in Fig. 5, but for $\theta = 40^\circ$. The fit for $n = 2$ and 3 is clearly inferior.

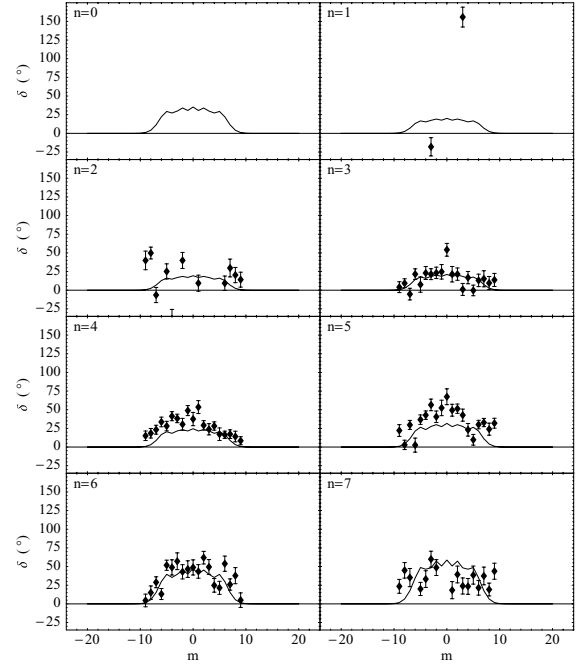


Figure 7. Same as in Fig. 5, but for $\ell = 205$.

cies (see the discussion associated with equation 4). On the other hand, the fit degrades comparatively slowly with increasing θ above 30° (see Fig. 6). Though $\theta = 30^\circ$ is clearly best, 40° may be judged acceptable. Of course, a real sunspot has a wide range of field inclinations, and attempting to model this with a single θ is bound to introduce inaccuracies.

The dependence on ℓ is addressed in Figs 7 and 8, with $\ell = 205$ and 411, respectively. At the lower ℓ , the fit is still quite good, and in particular the decrease in δ with decreasing ℓ is well modelled.

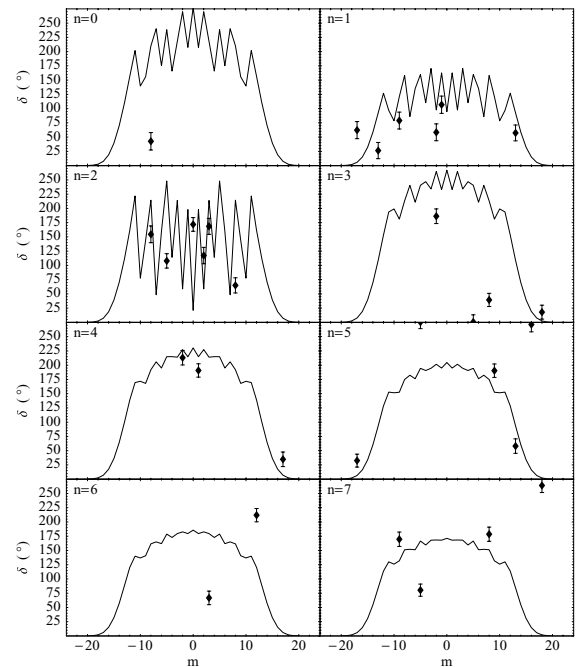


Figure 8. Same as in Fig. 5, but for $\ell = 411$. However, all phases have been shifted into the interval $(0^\circ, 360^\circ)$ in this case to avoid jumps when the model δ passes through 180° .

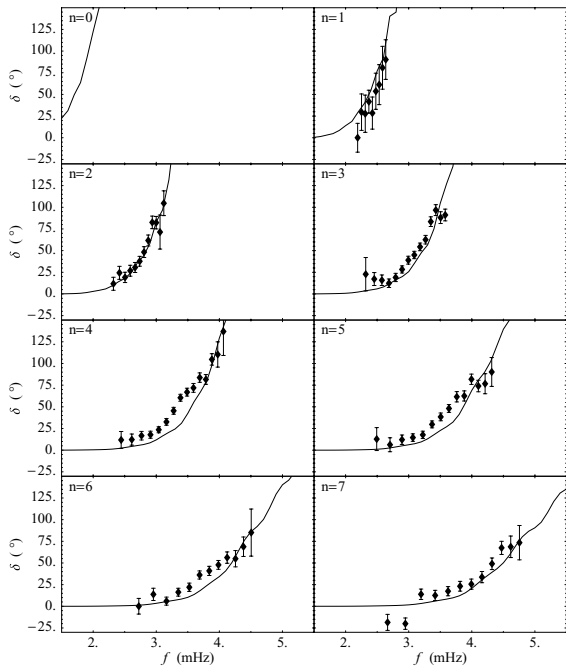


Figure 9. Phase shift δ (curve) as a function of frequency for the single-shell model with $L = 0.58$ Mm, $R = 27.5$ Mm, $\theta = 35^\circ$, and for axisymmetric oscillations ($m = 0$). The $n = 0$ panel corresponds to the f-mode, $n = 1$ to the p_1 -mode, etc. The plotted points are the m -averaged values for NOAA5254 Braun (1995), with only those points plotted that have estimated error bounds $\sigma_\delta \lesssim 30^\circ$. There are no f-mode points of this accuracy. Given the selected values of θ and R , the chosen L represents the least-squares best fit to the NOAA5254 phase shift data for p-modes $n = 1, \dots, 8$.

At the larger ℓ , the errors in the observational data are much larger, leaving very few ‘reliable’ points. There also appears to be more scatter, most notably at $n = 2$, which may reflect the highly spiky behaviour seen in the model curve, or may simply indicate that the data is highly unreliable. On the other hand, these higher ℓ -modes may be scattering off smaller-scale features in the spot.

Whereas modelling δ against m is fitted best with $L \approx 0.8$ Mm, fits of axisymmetric modes against frequency are optimized for somewhat smaller equipartition depths (and slightly larger θ , though this is less significant). Fig. 9 depicts phase shift versus frequency for $m = 0$ and the model $L = 0.58$ Mm, $R = 27.5$ Mm, $\theta = 35^\circ$, compared with the m -averaged δ for NOAA5254. As discussed in Braun (1995), δ is averaged over a small range of m about 0 in order to reduce errors and scatter. The m range varies, but is chosen so as to not intrude far into the ‘shoulders’ seen in previous figures. Given the limitations of the model discussed earlier, the qualitative agreement in behaviour is pleasing. Better agreement with individual p-mode ridges can be obtained by slightly varying parameters; e.g. reducing L to 0.55 Mm brings the p_1 ridge into almost perfect agreement, though at the expense of the accuracy of the $n \gtrsim 4$ curves. On the other hand, raising L to 0.8 Mm as in previous figures produces comparatively poor results for lower n . Specifically, the ridges are shifted too far to the left (recall that frequency scales as $L^{-1/2}$), though their slopes remain approximately correct. This is clearly a residual effect of the mispositioning of the p-mode ridges by the polytropic model. It is anticipated that moving to a model based on realistic solar structure instead of a polytrope would improve the match significantly.

Previous attempts to model p-mode absorption in sunspots based on slow-mode conversion and vertical magnetic fields have

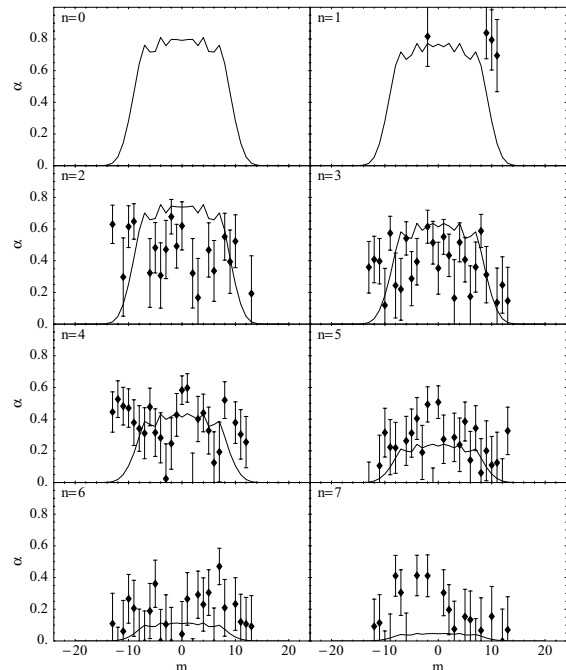


Figure 10. Absorption coefficient α versus azimuthal order m for various radial orders n for the model $L = 0.8$ Mm, $R = 27.5$ Mm, $\theta = 40^\circ$ and waves with $\ell = 288$.

founded on the seeming impossibility of obtaining sufficient absorption beyond the f- and perhaps p_1 -modes. However, with inclined field, absorption is ample! Fig. 10 shows α as a function of m for the case $L = 0.8$ Mm, $R = 27.5$ Mm, $\theta = 40^\circ$. Plotting α as a function of frequency (Fig. 11) reveals a similar picture.

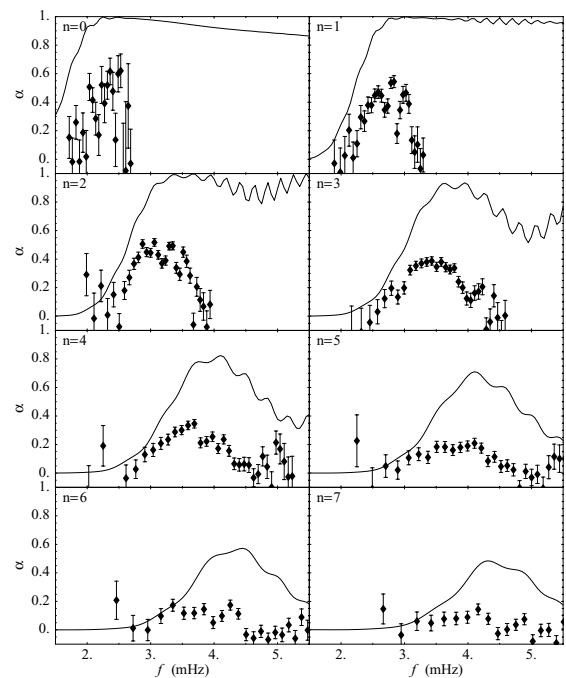


Figure 11. Absorption coefficient α versus frequency for the case of Fig. 9. Again the comparison is with m -averaged Hankel data. Error bars have been suppressed in the interests of clarity, but only those points with $\sigma_\alpha < 0.15$ have been retained.

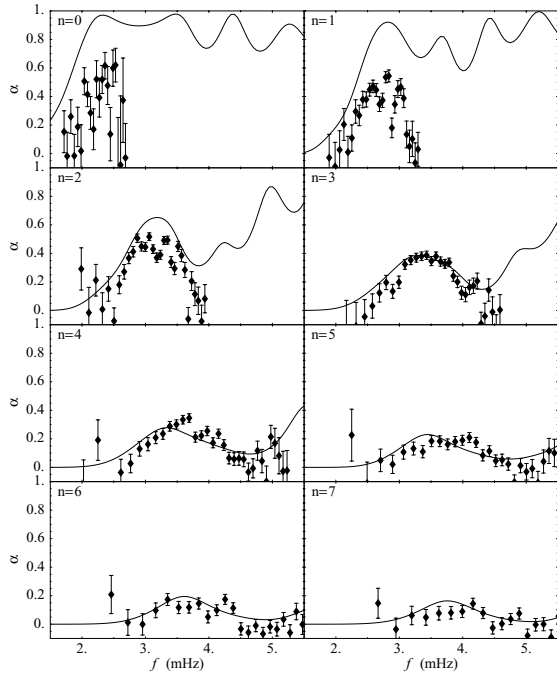


Figure 12. Absorption coefficient α versus frequency for $\theta = 35^\circ$, $L = 0.85$ Mm, and $R = 9$ Mm.

Correspondence of the model curves with the dip at 5 mHz may be improved by increasing L (see Fig. 12).

Several points should be made concerning Figs 11 and 12. First, there is a minimum in α corresponding to the first dip in the $\text{Im}(\kappa)$ curves (see Fig. 3). Although this dip does not extend to zero for $\theta \neq 0$ as it does in the vertical field case (Cally et al. 1994), it is none the less substantial (note the logarithmic scale in the figure). At these frequencies, the coupling of fast and slow modes is weak, especially at high radial order. Since $f \propto v/\sqrt{L}$, the dip may be moved around in frequency by varying L . If it is believed that the dip in absorption in the Hankel data is actually due to this effect, this gives us a means of fixing L . This is how L was chosen for Fig. 12. Indeed, the tendency for the dip to occur at lower frequency for low radial orders n (most clearly seen in Fig. 2) is matched here.

However, evidence from acoustic holography suggests that the 5-mHz dip may instead be due to an enhancement of emission in this frequency band in a region (the acoustic glory) surrounding the spot (Donea et al. 2000; Jain & Haber 2002). Nevertheless, the correspondence between the 5-mHz dip and the $\text{Im}(\kappa)$ dip at just about the right L seems too great a coincidence to ignore, and we might be led to believe that both mechanisms are at work here.

Even with the $\text{Im}(\kappa)$ dip though, the absorption produced by the model at higher frequencies and low radial order is far too great. A much smaller absorbing radius R can partially rectify this (see Fig. 12), though the discrepancy at low n and large f is still problematic. Cally et al. (1994) argued, in the case of the f-mode, that dissipative mechanisms operate at these frequencies (associated with interaction between the wave and convection), which cause high-frequency modes to be local rather than global in nature. The ‘memory’ of the nearby absorbing spot is therefore rapidly dissipated. The presence of the acoustic glory only amplifies this effect. These mechanisms are not easily modelled at the fundamental level, but reasonable ad hoc prescriptions appear capable of substantially reducing the excess absorption. Another possible cause is our neglect

of the dependence of $\text{Im}(\kappa)$ on the angle ϕ at which the waves meets the vertical plane containing the magnetic field vector \mathbf{B} . Although as mentioned earlier, our model assumes no dependence on ϕ , in reality $\text{Im}(\kappa)$ does noticeably decrease with frequency for p-modes in field with $\theta \approx 30^\circ$ and $\phi \approx 90^\circ$, in contrast to its behaviour at $\phi = 0^\circ$ (Fig. 3).

A final possible reason for the excess absorption in the modes, and possibly the most important one, is that absorption peaks rather sharply around $\theta = 30^\circ$ in the Crouch & Cally (2003) results (see fig. 9 of that paper, noting the logarithmic scale), whereas phase shift [i.e. $\text{Re}(\kappa)$] varies more gradually. Consequently, whilst an average phase shift associated with $\theta \approx 30^\circ$ does a good job of representing the whole spot, applying this angle everywhere substantially overestimates absorption, which in reality occurs predominantly in regions with that field inclination. This would explain why the absorption versus frequency curves are too high for parameters optimized to fit phase shift data, despite having the right general shape.

The oscillations particularly evident in the p_1, \dots, p_4 curves in Fig. 11 are due to leaky resonances in the spot, i.e. partial reflections at $r = R$. Since real sunspots may not have such sharp boundaries, this effect may be smeared in practice.

3.2 Multiple shell models

The impact parameter shoulder in the α versus m Hankel data (Fig. 10) is far less clear than it is in δ . This suggests that the absorbing region is actually more extended in radius than is the phase shift region. This is consistent with the result that plage produces a measurable absorption but effectively no phase shift in the Hankel data (Braun 1995). Consequently, we might expect the diffuse magnetic elements surrounding sunspots to continue absorbing beyond the scattering region.

The tendency for δ to be negative for low frequencies when $\theta < 30^\circ$, mentioned in Section 2, suggests that the umbral core, where the

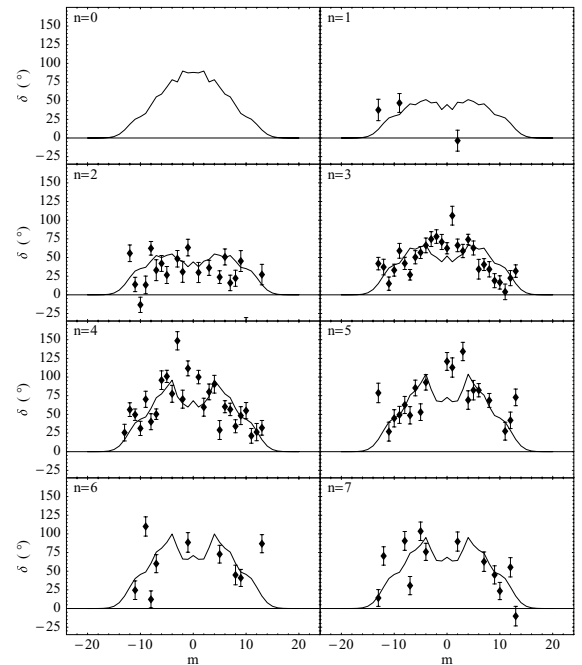


Figure 13. Phase shift δ versus azimuthal order m for various radial orders n for the multishell model $L = \{1, 1, 0.8, 0.6, 0.4\}$ Mm, $R = \{6, 9, 18, 25, 35\}$ Mm, and $\theta = \{0^\circ, 20^\circ, 30^\circ, 40^\circ, 55^\circ\}$, and waves with degree $\ell = 288$.

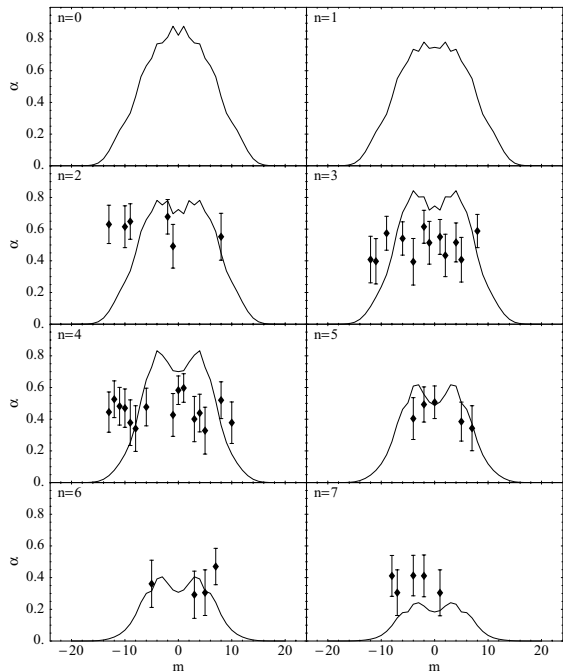


Figure 14. Absorption coefficient α versus azimuthal order m for the five-shell model of Fig. 13, again with $\ell = 288$.

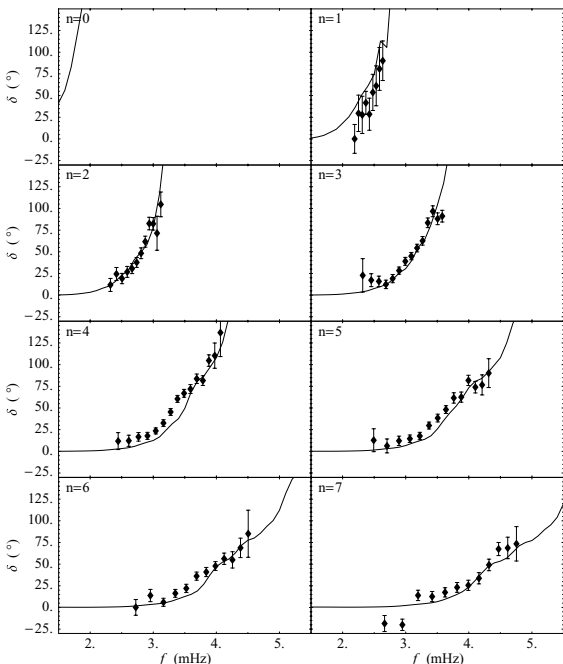


Figure 15. Phase shift δ versus frequency for the five-shell model of Fig. 13.

field is presumably close to vertical, should show up as a dip in the δ versus m graphs at low impact parameter, i.e. low m . Although there is some hint of this in the observational Hankel data for individual m , the scatter makes it unclear whether the effect is really there. Similar comments can be made about α , since it too is greatly reduced in the vertical field.

On the one hand, the lack of a shoulder in the α versus m Hankel data suggests that the absorbing region is large, but on the other hand,

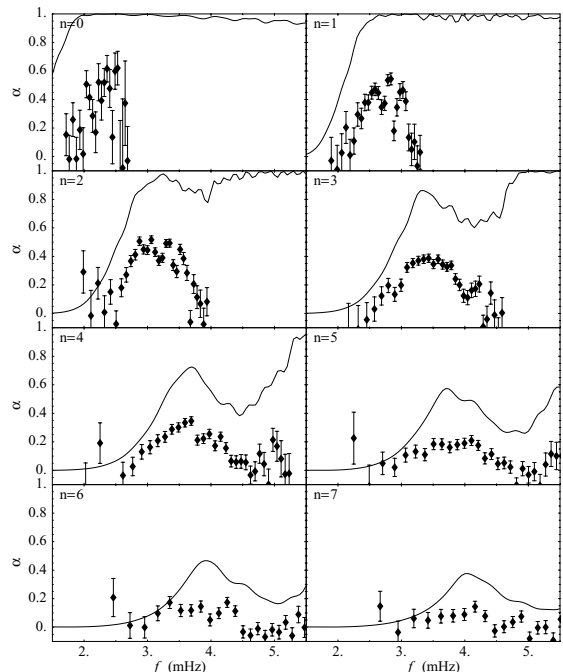


Figure 16. Absorption coefficient α versus frequency for the five-shell model of Fig. 13.

α versus frequency graphs (Fig. 12) produce best results for small $R!$ Seemingly, one way around this conundrum is to suppose that absorption occurs predominantly in a comparatively thin shell at large radius, thereby presenting a wide target to incoming waves, whilst at the same time not absorbing them too much. Alternatively, acoustic glories and finite mode lifetime effects may bring the absorption graphs into line with observations without the need to reduce R .

With that point in mind, Fig. 13 displays δ for $\ell = 288$ and a five-shell model consisting of a range of L and θ values. The dips created by the ‘umbra’ are evident in the model curves. Unfortunately, the quality of the Hankel data is insufficient to usefully probe the umbra in this way. Nevertheless, this somewhat arbitrary model indicates some of the features of a multishell scenario. Figs 13–16 further illustrate the character of this particular five-shell model. Overall, it yields a good fit to the phase shift data, and at least a qualitatively correct fit to the absorption data, though as usual α is a little too high and the α shoulder too narrow in m . It would seem that the absorbing area for the NOAA5254 spot exceeds 35 Mm, which takes it well into the Hankel annulus.

4 CONCLUSIONS

In this paper, we have explored the consequences of modelling sunspot absorption and phase shift in a crude way using the tabulated eigenvalues of Crouch & Cally (2003). Overall, given the simplifications made, the correspondence between observational Hankel data and the models is very impressive, especially for δ . Indeed, it is remarkable that the phase shift data can be fitted so well using just magnetic effects, without including internal/external thermal differences.

Subsurface thermal perturbations have been a major focus of tomographic (time–distance) studies in recent years. For sunspots, Kosovichev et al. (2000) (see also Kosovichev 2002) report a typical 0.3–1 km s⁻¹ increase in ray-speed in a region as broad as the

surface spot and some 10 Mm deep beneath it. As a comparison, the quiet sun speed of sound is around 20 km s^{-1} at 4 Mm deep, and 37 km s^{-1} at 10 Mm. They cannot distinguish between sound and fast mode speed, but estimate that it would correspond to a field strength of 18 kG if the increase were entirely magnetic. Given the total sunspot surface magnetic flux though, an 18 kG field at these depths should not fill such a broad region, so we may assume the effect to be mostly thermal. However, also, judging from their fig. 8, there is a wave speed decrease in the first 2–3 Mm beneath the spot, consistent with the spot being cooler than its surrounds in the surface layers. The fact that p-modes actually speed up as they pass through a spot, indicated by their positive phase shifts, and that the models presented here yield excellent agreement with these observed shifts despite thermal perturbations being ignored, suggests that the increase in p-mode phase speeds is predominantly due to magnetoacoustic coupling at shallow depths (less than 1 Mm) rather than deep thermal perturbations. However, the linkage between the modal and ray descriptions is quite complex (Bogdan 1997), and the comparison between them is far from straightforward.

Absorption α in our models is consistently somewhat high for values of the parameters L , θ and R , which produce good phase shift fits, though qualitative behaviour is a good match. The discrepancy could be due to several causes, most notably:

- (i) inappropriately applying a $\theta \approx 30^\circ$ model, for which absorption is strongly peaked, everywhere in the spot;
- (ii) the neglect of convective mode dissipation, depressed acoustic emission inside spots and enhanced acoustic emission surrounding spots;
- (iii) due to a sunspot field not being uniform as in the model, the effective magnetic field strength at depths where phase shifting and absorption happen may be quite different, meaning that different parameters may be required in modelling each of the two effects.

Typically, good results are obtained with equipartition depth L between 600 and 800 km roughly, corresponding to Alfvén and speed of sounds at $z = -L$ of around 10–11 km s^{-1} or magnetic field strengths of 3.6–4.8 kG. These are very reasonable numbers.

Indeed, overall, we have been very successful in addressing the list of points set out at the end of Section 1, as well as others relating to variation with m . However, the polytropic model adopted here is too crude to warrant detailed comparisons with a view to quantitative inversions. It particularly affects the horizontal positioning of curves representing α or δ against frequency. It would be useful to recalculate the Crouch & Cally tables for a realistic solar model, and to reapply the procedures developed here to them. However, this is not trivial. Although the eigenvalue differential equations are solved numerically using a shooting method, the eigenvalues rely crucially on the analytic asymptotic solution of the equations for large depth and to high order. This is done using a dominant balance method (which incidentally relies on $4m_p$ being an integer), and it is not clear how to carry this over to a general (tabulated) model. In practice, replacing the solar model by a polytrope below some depth is probably the best way to proceed. Even with a realistic solar model though, the neglect of field strength variation with depth, and thermal differences inside the spot, could preclude an exact comparison.

Unfortunately, the task of calculating eigenvalues for more complex magnetic geometries is mathematically extremely difficult.

Perhaps the most pertinent lesson to be drawn from our results is that slow mode conversion does indeed seem to be the predominant mechanism responsible for the observed absorption and phase shifts. And in particular, an inclined magnetic field is necessary to make the process work.

ACKNOWLEDGMENTS

PSC wishes to acknowledge the hospitality of the High Altitude Observatory where this work was carried out during a visit in 2003. DCB is supported by awards AST-9987286 from the National Science Foundation, and awards NASW-01007 and NAG5-12901 from the National Aeronautics and Space Administration.

REFERENCES

- Barnes G., Cally P.S., 2000, *Solar Phys.*, 193, 373
 Barnes G., Cally P.S., 2001, *Publ. Astron. Soc. Aust.*, 18, 243
 Bogdan T.J., 1997, *ApJ*, 477, 475
 Bogdan T.J., Cally P.S., 1995, *ApJ*, 453, 919
 Bogdan T.J., Cally P.S., 1997, *Proc. R. Soc. Lond. A*, 453, 943
 Bogdan T.J., Brown T.M., Lites B.W., Thomas J.H., 1993, *ApJ*, 406, 723
 Braun D.C., 1995, *ApJ*, 451, 859
 Braun D.C., Duvall T.L., LaBonte B.J., 1987, *ApJ*, 319, L27
 Braun D.C., Duvall T.L., LaBonte B.J., Jefferies S.M., Harvey J.W., Pomerantz M.A., 1992, *ApJ*, 391, L113
 Braun D.C., Lindsey C., 2000a, *Solar Phys.*, 192, 285
 Braun D.C., Lindsey C., 2000b, *Solar Phys.*, 192, 307
 Cally P.S., 1983, *Solar Phys.*, 88, 77
 Cally P.S., 2000, *Solar Phys.*, 192, 395
 Cally P.S., Bogdan T.J., 1993, *ApJ*, 402, 732
 Cally P.S., Bogdan T.J., Zweibel E.G., 1994, *ApJ*, 437, 505
 Crouch A.D., Cally P.S., 2003, *Solar Phys.*, 214, 201
 Chou D.-Y., 2000, *Solar Phys.*, 192, 241
 Christensen-Dalsgaard J., 1997, Aarhus adiabatic pulsation package, <http://astro.phys.au.dk/~jcd/adipack/n/>
 Donea A.-C., Lindsey C., Braun D.C., 2000, *Solar Phys.*, 192, 321
 Fan Y., Braun D.C., Chou D.-Y., 1995, *ApJ*, 451, 877
 Hunter J.P., 1999, PhD thesis, Monash University
 Jain R., Haber D., 2002, *A&A*, 387, 1092
 Kosovichev A.G., 2002, *Astron. Nachr.*, 323, 186
 Kosovichev A.G., Duvall T.L. Jr, 1997, in Christensen-Dalsgaard J., Pijpers F., eds, *Astrophys. Space Sci. Lib.*, 225, SCORe'96: Solar Convection and Oscillations and their Relationship. Kluwer, Dordrecht, p. 241
 Kosovichev A.G., Duvall T.L. Jr, Scherrer P.H., 2000, *Solar Phys.*, 192, 159
 Kosovichev A.G., Duvall T.L. Jr, Scherrer P.H., 2001, in Mathys G., Solanki S.K., Wickramasinghe D.T., eds, *ASP Conf. Ser.*, Vol. 248, *Magnetic Fields across the Hertzsprung–Russell Diagram*. Astron. Soc. Pac., San Francisco, p. 139
 Lindsey C., Braun D.C., 1999, *ApJ*, 510, 494
 Scheuer M.A., Thomas J.H., 1981, *Solar Phys.*, 71, 21
 Spruit H.C., 1991, in Toomre J., Gough D.O., eds, *Lecture Notes in Physics*, Vol. 388, *Challenges to Theories of the Structure of Moderate Mass Stars*. Springer-Verlag, Berlin, p. 121
 Spruit H.C., Bogdan T.J., 1992, *ApJ*, 391, L109
 Zhang H., 1997, *ApJ*, 479, 1012

This paper has been typeset from a $\text{\TeX}/\text{\LaTeX}$ file prepared by the author.